



ARL-TR-7783 • SEP 2016



Characterization of Magnetron Sputtered Copper-Nickel Thin Films and Alloys

by Eugene Zakar, Andrew Chen, Robert Burke,
Samuel G Hirsch, Nicholas Strnad, and James Mulcahy

NOTICES

Disclaimers

The findings in this report are not to be construed as an official Department of the Army position unless so designated by other authorized documents.

Citation of manufacturer's or trade names does not constitute an official endorsement or approval of the use thereof.

Destroy this report when it is no longer needed. Do not return it to the originator.



Characterization of Magnetron Sputtered Copper-Nickel Thin Films and Alloys

by Eugene Zakar, Andrew Chen, and Samuel G Hirsh
Sensors and Electron Devices Directorate, ARL

Robert Burke, Nicholas Strnad, and James Mulcahy
General Technical Services, LLC, Columbia, MD

REPORT DOCUMENTATION PAGE				Form Approved OMB No. 0704-0188	
<p>Public reporting burden for this collection of information is estimated to average 1 hour per response, including the time for reviewing instructions, searching existing data sources, gathering and maintaining the data needed, and completing and reviewing the collection information. Send comments regarding this burden estimate or any other aspect of this collection of information, including suggestions for reducing the burden, to Department of Defense, Washington Headquarters Services, Directorate for Information Operations and Reports (0704-0188), 1215 Jefferson Davis Highway, Suite 1204, Arlington, VA 22202-4302. Respondents should be aware that notwithstanding any other provision of law, no person shall be subject to any penalty for failing to comply with a collection of information if it does not display a currently valid OMB control number.</p> <p>PLEASE DO NOT RETURN YOUR FORM TO THE ABOVE ADDRESS.</p>					
1. REPORT DATE (DD-MM-YYYY) September 2016		2. REPORT TYPE Technical Report		3. DATES COVERED (From - To) 10/2015 to 7/2016	
4. TITLE AND SUBTITLE Characterization of Magnetron Sputtered Copper-Nickel Thin Film and Alloys				5a. CONTRACT NUMBER	
				5b. GRANT NUMBER	
				5c. PROGRAM ELEMENT NUMBER	
6. AUTHOR(S) Eugene Zakar, Andrew Chen, Robert Burke, Samuel G Hirsch, Nicholas Strnad, and James Mulcahy				5d. PROJECT NUMBER	
				5e. TASK NUMBER	
				5f. WORK UNIT NUMBER	
7. PERFORMING ORGANIZATION NAME(S) AND ADDRESS(ES) US Army Research Laboratory ATTN: RDRL-SER-L 2800 Powder Mill Road Adelphi, MD 20783-1138				8. PERFORMING ORGANIZATION REPORT NUMBER ARL-TR-7783	
9. SPONSORING/MONITORING AGENCY NAME(S) AND ADDRESS(ES)				10. SPONSOR/MONITOR'S ACRONYM(S)	
				11. SPONSOR/MONITOR'S REPORT NUMBER(S)	
12. DISTRIBUTION/AVAILABILITY STATEMENT Approved for public release; distribution is unlimited.					
13. SUPPLEMENTARY NOTES					
14. ABSTRACT Copper (Cu)-nickel (Ni) thin films are prepared by magnetron sputtering using an AJA International model ATC-2200 system. The as-deposited films are in the amorphous state during room temperature deposition but transition to a crystalline state at an elevated substrate temperature beyond 250 °C. The crystalline films have a mixed (111)- and (200)-oriented texture that becomes predominantly (111)-orientated after an annealing treatment. Bilayer CuNi deposited films with ratio of 12:1, 6:1, 4:1, and 3:1 produced final alloy concentrations of 90/10, 83/17, 76/24, and 70/30 atomic %, respectively, after annealing, and their average surface roughness increased with higher Cu concentration. These results show that the final thin film alloy composition can be effectively controlled by varying the ratio of the initial deposited Cu and Ni layers. The morphology of these films were studied by atomic force microscope (AFM), X-ray Diffraction (XRD), electrical 4-point probe, and energy-dispersive X-ray spectroscopy (EDX).					
15. SUBJECT TERMS CuNi alloy, deposition, sputter, thin film, LPCVD					
16. SECURITY CLASSIFICATION OF:			17. LIMITATION OF ABSTRACT UU	18. NUMBER OF PAGES 18	19a. NAME OF RESPONSIBLE PERSON Eugene Zakar
a. REPORT Unclassified	b. ABSTRACT Unclassified	c. THIS PAGE Unclassified			19b. TELEPHONE NUMBER (Include area code) (301) 394-1628

Contents

List of Figures	iv
List of Tables	iv
1. Introduction	1
1.1 Co-sputter Deposition	1
1.2 Experimental Parameters	1
1.2.1 Sample Preparation	1
2. Experimental Results	3
2.1 Sputter deposition rates for Cu and Ni films	3
2.2 Effect of Argon Chamber Pressure During Sputtering	4
2.3 Effect of Substrate Temperature During Sputtering	5
2.4 XRD texture Analysis of As-deposited CuNi Bilayer and Alloyed Films	6
2.5 Composition Analysis of the Alloyed Films	6
2.6 Effect of Composition on Surface Roughness	7
2.7 Uniformity of the Depositions	8
3. Conclusion	9
4. References and Notes	10
List of Symbols, Abbreviations, and Acronyms	11
Distribution List	12

List of Figures

Fig. 1	Plot of deposition rates for a) Ni and b) Cu sputtered films	4
Fig. 2	XRD of as-deposited films showing effect of a) sputter pressure on Cu at 25 °C and b) substrate temperature on Ni at 5 mT	5
Fig. 3	XRD texture of CuNi bilayer and alloyed films	6
Fig. 4	AFM image and roughness measurement of a) 220 nm for 12:1, b) 86 nm for 6:1, c) 74 nm for 4:1, and d) 66 nm for 3:1 CuNi alloy....	8
Fig. 5	Contour map showing measured electrical resistivity values across 25 points on a 100-mm diameter substrate for 3:1 CuNi alloy.....	8

List of Tables

Table 1	Experimental sputtering parameters	2
Table 2	List of prepared bilayer CuNi samples	3
Table 3	EDX composition analysis of the CuNi alloyed films.....	7

1. Introduction

1.1 Co-sputter Deposition

Sputter coating is the process of creating a vapor via physical means and depositing the vapor to form a thin film on a substrate. Sputtering uses ions from a gas discharge plasma in an electric field. The electric field accelerates the ions towards the target material, the cathode. The resulting collision and transfer of kinetic energy dislodges atoms from the target, which then impinge on the substrate—the anode—forming the desired thin film.¹ Sputtering sources often employ an arrangement of permanent magnets, or magnetrons, that use strong electric and magnetic fields to confine charged plasma particles near the surface of the sputter target. Electrons follow helical paths around magnetic field lines undergoing more ionizing collisions with gaseous neutrals near the target surface. The magnetron configuration allows a higher sputtering rate than targets without the magnetron configuration.

The amount of material sputtered, Q , in a unit of time under constant conditions is inversely proportional to the gas pressure, p , and anode-cathode distance, d :

$$Q = k V I / p d \quad (1)$$

where k is the constant of proportionality, V is the working distance, and I is the discharge current.

Co-sputtering can be performed by using 2 targets, either simultaneously or by alternating the 2 targets. Co-sputtering is used to form alloys or deposit composite materials. The stoichiometry is controlled by optimizing the power density of each gun (target) separately. In this report, we describe a modified co-sputtering process whereby a first layer of nickel (Ni) thin film is deposited on the substrate, followed by a second layer of copper (Cu) thin film that forms an alloy after a high-temperature anneal process.

1.2 Experimental Parameters

1.2.1 Sample Preparation

We used an AJA International Inc. model ATC-2200 sputter system with 75-mm-diameter targets in a Stiletto Series ST30 source configuration. Options on the system include the ability to adjust the substrate distance, tilt the target, and heat the substrate.

Prior to preparation of the CuNi bilayer, it was necessary to determine the deposition rates for Cu and Ni in order to precisely control each film thickness. Initial deposition rate studies of Cu and Ni were carried out on a 100-mm wafer. Uniformity should not be an issue, since the sputter system was designed to provide good uniformity across a substrate twice the target diameter. Keeping in mind that the uniformity of the film improves if the chamber pressure is decreased and/or the distance between target and substrate is increased, we decided to set the distance to 100 mm. For this study, we chose to vary the argon (Ar) pressure and the substrate temperature during sputtering. Power, target to substrate distance, target tilt angle, and substrate rotation were held constant. A summary of our experimental sputtering parameters is found in Table 1. In theoretical terms the amount of sputtered material, Q , is inversely proportional to the substrate distance, d , from the source target according to Eq. 1. In order to make up for the reduction in Q due to the high d , we intentionally increased the power level to a relatively high level of 500 W d.c. to improve the deposition rate in order to achieve a film thickness of 1 μm within a reasonable amount of time. Substrate rotation was employed during the sputtering to improve the uniformity of the film across the diameter of the substrate.

Table 1 Experimental sputtering parameters

Parameter	Const/Var	Condition (unit)
Power	Constant	500 (W d.c.)
Distance	Constant	100 (mm)
Target tilt	Constant	6 (mm)
Rotation	Constant	60 (rot/min)
Ar pressure	Variable	5, 10, 15 (mT)
Substrate temp.	Variable	25, 250, 400 ($^{\circ}\text{C}$)

The starting substrate material consisted of a polished silicon (Si) wafer—500 μm thick, 100 mm in diameter with (100) orientation, N-doped, and a 280-nm layer of thermal oxide grown on top. After loading the sample and evacuating the sputter chamber to a base pressure of $\sim 10^{-7}$ Torr, the experiments were performed in the presence of different Ar gas pressure and temperature settings for each sample with a deposition time of 5 min. After a deposition was complete, the substrate was coated with photoresist and exposed to a wet etchant to remove the Cu or Ni film from a portion of the wafer in order to measure the film thickness. The film thickness was measured using a Tencor KLA-15 profilometer. The deposition rate was calculated by taking the measured film thickness and dividing by the deposition time. A plot of the calculated deposition rates for Cu and Ni was then generated for the variable deposition parameters.

Based on the derived deposition rates, we then proceeded to prepare several bilayer thin film samples with different thickness ratios of Cu to Ni (Table 2). Varying amounts of Ni (50, 100, 150, and 200 nm) were sputter-deposited on the starting wafer, followed by a fixed 600-nm layer of Cu on top. The bilayer stacks were then annealed for 30 min at 1000 °C in the presence of 40% H₂/60% Ar gas mixture at a pressure of 15 Torr to form alloys of varying concentrations that were later confirmed by the energy-dispersive X-ray spectroscopy (EDX) method.

Table 2 List of prepared bilayer CuNi samples

Sample No.	CuNi ratio	Layer Thickness (nm)	Temp (°C)	Pressure (mT)
S1	12:1	(600nmCu:50nmNi)	25	5
S2	12:1	(600nmCu:50nmNi)	25	15
S3	12:1	(600nmCu:50nmNi)	400	5
S4	12:1	(600nmCu:50nmNi)	400	15
S5	6:1	(600nmCu:100nmNi)	25	5
S6	6:1	(600nmCu:100nmNi)	25	15
S7	6:1	(600nmCu:100nmNi)	400	5
S8	6:1	(600nmCu:100nmNi)	400	15
S9	4:1	(600nmCu:150nmNi)	25	5
S10	4:1	(600nmCu:150nmNi)	25	15
S11	4:1	(600nmCu:150nmNi)	400	5
S12	4:1	(600nmCu:150nmNi)	400	15
S13	3:1	(600nmCu:200nmNi)	25	5
S14	3:1	(600nmCu:200nmNi)	25	15
S15	3:1	(600nmCu:200nmNi)	400	5
S16	3:1	(600nmCu:200nmNi)	400	15

Characterization of the as-deposited bilayer films and post-annealed CuNi alloys was accomplished by an X-ray diffraction (XRD) Rigaku system with CuK α radiation, $\lambda=0.15405$ nm, in the Bragg-Brentano geometry, and the sealed X-ray source tube was operating at 40 kV and 44 mA current. Surface morphology was investigated by an atomic force microscopy (AFM) Veeco Nanoman system. The microstructural and elemental compositions of the final alloyed films were analyzed using EDX.

2. Experimental Results

2.1 Sputter Deposition Rates for Cu and Ni Films

The deposition rates for Cu and Ni with respect to Ar pressure are shown in Figs. 1a and b. The differences in the sputter deposition rates for Cu and Ni can be attributed to the differences in the mass for Cu and Ni atoms. Based on the data, pressure had a significant effect on the sputter rates. The sputter rate for Ni increased from 198 to 230 Å/min when there was a reduction in pressure from

15 to 5 mT at 25 °C. The sputter rate for Cu increased from 336 to 451 Å/min when there was a reduction in pressure from 15 to 5 mT. The substrate temperature did not appear to greatly influence the sputter rate at 5 mT pressure for either of the target materials, as shown in the plots. The sputter rate for Ni only increased by 6 Å/min when the substrate temperature was increased from 25 to 400 °C. The Cu sputter rate increased by 10 Å/min with the same rise in temperature.

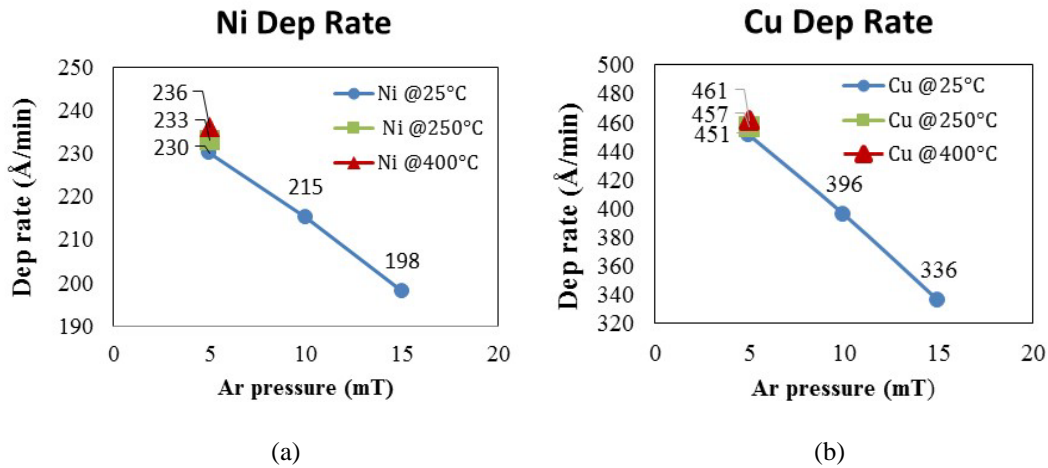


Fig. 1 Plot of deposition rates for a) Ni and b) Cu sputtered films

2.2 Effect of Argon Chamber Pressure during Sputtering

Pressure had a significant effect on the sputter rates for both Cu and Ni samples according to the results from Fig. 1. The sputter rates for Cu and Ni increased when the pressure decreased from 15 to 5 mT at 25 °C. The increase in the sputtering rate is due to the decreased pressure in the chamber that leads to fewer collisions between Ar atoms in the plasma, allowing more sputtered atoms to reach the surface of the substrate. The effect of Ar pressure on the nature of the XRD diffraction patterns for as-deposited Cu film is shown in Fig. 2a. There are 2 major intensity peaks for Cu—a (111) peak at 2θ position of 44.6° and a (200) peak at 2θ position of 50.6° . The intensity of the (111) and (200) peaks increased when there was a reduction in Ar pressure, while at the same time each of the peaks became narrower and sharper. The same effect was seen with sputter-deposited Ni film samples (not shown). A low Ar pressure setting of 3 mT produced the highest intensity peak and sputter rates for the Cu- and Ni-deposited films. However, due to the unsteady nature of the plasma occurring at the low 3-mT setting, we discontinued its use and maintained a 5-mT setting for the rest of the experiments.

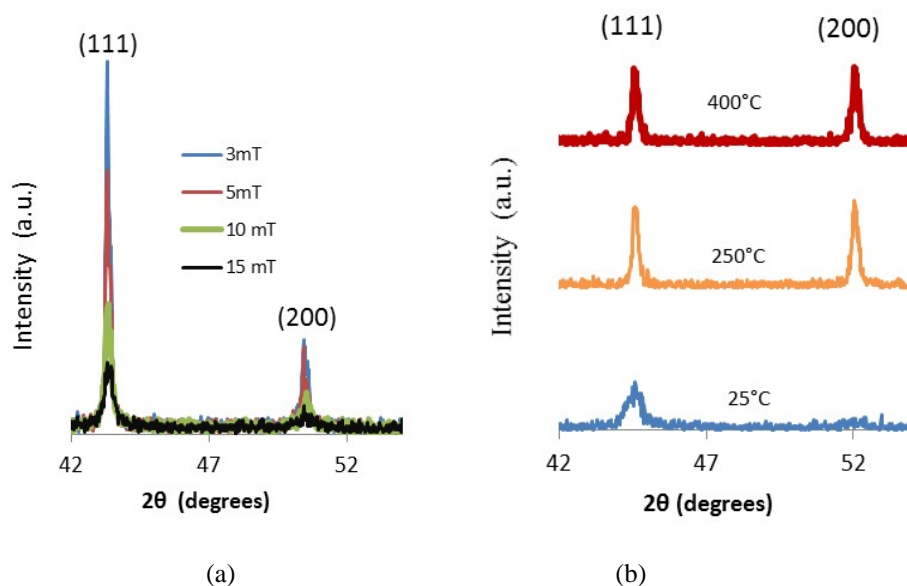


Fig. 2 XRD of as-deposited films showing effect of a) sputter pressure on Cu at 25 °C and b) substrate temperature on Ni at 5 mT

2.3 Effect of Substrate Temperature during Sputtering

The substrate temperature had a significant effect on the crystallinity of the deposited films. Figure 2b shows the XRD peaks of a non-crystalline Ni film deposited at a substrate temperature of 25 °C and 5 mT. Its 2θ peak intensity of (111) texture at 44.6° looks approximately equal in proportion to its width. There appears to be a little bump at the 2θ position of 52.1° , which is a typical characteristic of an amorphous layer. Amorphous, or non-crystalline, film is observed when the X-rays are scattered in many directions, leading to a bump-like feature across the 2θ position instead of a narrow and high peak.³ A crystalline film is typically composed of highly ordered and periodically arranged atoms in a 3-D space. The transition from an amorphous film to a crystalline film was clearly attained at higher sputter substrate temperatures of 250 and 400 °C for the Ni film, as evidenced from the XRD peaks becoming sharper and narrower. The same results are observed for the sputtered Cu film samples. The additional appearance of (220) and (311) peaks became noticeable (not show here) when the sputtering pressure was increased above 15 mT.²

Since only (111) textured grains are desired in this experiment, we decided to narrow our choice of samples to S3, S7, S11, and S15, as they fall within the most favorable parameters of 400 °C substrate temperature and 5-mT Ar chamber pressure according to Table 2.

2.4 XRD texture Analysis of As-Deposited CuNi Bilayer and Alloyed Films

We studied the evolution of film texture from the as-deposited condition of Cu, Ni, and CuNi bilayer films to the final alloying stage. The XRD patterns for individual as-deposited Cu and Ni films with (111) and (200) peaks, including the co-deposited CuNi bilayer and alloyed film for sample S3, are shown in Fig. 3. The Cu and Ni films in this figure were deposited at the optimized deposition pressure of 5 mT and temperature of 400 °C. The 3:1 Cu:Ni bilayer films have the additive characteristics of the individual Cu and Ni peaks. When the co-deposited bilayer films were finally annealed at 1000 °C for 30 min, the final 3:1 CuNi alloy transformed to a preferred (111) orientation. There is a slight shift in the 2θ position of the (111) peak to a higher angle, which indicates the formation of the alloyed film, with the Ni substituting the lattice sites of Cu since the ionic radius of Ni (69 pm) is lower than that of Cu (72 pm). We observed similar behavior in the other samples of Cu and Ni with ratios of 4:1, 6:1, and 12:1, with the exception that bilayer films 3:1 sputtered at a low temperature of 25 °C, which produced undesirable non-crystalline films.

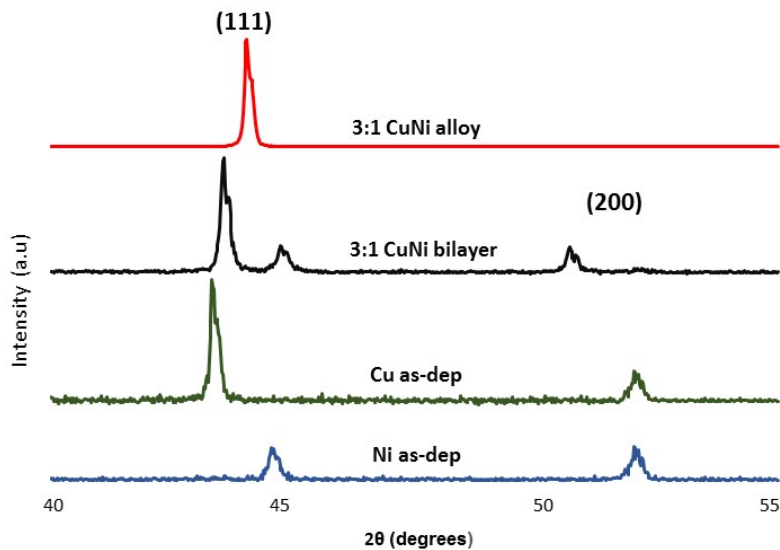


Fig. 3 XRD texture of CuNi bilayer and alloyed films

2.5 Composition Analysis of the Alloyed Films

EDX spectroscopy is an analytical technique used for the elemental analysis or chemical characterization of samples. The EDX parameters used here were a 20-kV accelerating voltage, 104-μA beam current, 10k counts on the Cu k range, and 2000x magnification on each of the samples.

Several samples sputtered at a high substrate temperature of 400 °C and low pressure of 5 mT, which previously showed preferred (111) crystalline structures were alloyed for EDX analysis. The results of the alloy concentration analysis are reported in Table 3 in terms of both the atomic % (at.%) and weight %. Bilayer films consisting of Cu to Ni ratios of 12:1, 6:1, 4:1, and 3:1 produced alloy concentrations of 90/10, 82/18, 76/24, 71/29 at.%, respectively, after annealing. Samples with the 6:1 and 4:1 ratios may have deviated from the expected ideal 80/20 at.% and 75/25 at.% by approximately ± 1 at.% due to slight differences in the actual deposited layer thickness of the bilayer films.

Table 3 EDX composition analysis of the CuNi alloyed films

Cu:Ni ratio	CuNi layer thickness (nm)	Alloy concentration	
		(at.%)	(weight %)
12:1	600Cu/50Ni	90Cu/10Ni	91Cu/09Ni
6:1	600Cu/100Ni	82Cu/18Ni	83Cu/17Ni
4:1	600Cu/150Ni	76Cu/24Ni	77Cu/23Ni
3:1	600Cu/200Ni	70Cu/30Ni	71Cu/29Ni

2.6 Effect of Composition on Surface Roughness

The CuNi bilayer deposited films were annealed for 30 min at 1000 °C in a low-pressure chemical vapor deposition (LPCVD) reactor with a gas mixture of 40%H₂/60%Ar at 15 Torr pressure to form the final alloys. We measured the average roughness (R_a) of the annealed films using AFM over an area consisting of 20 × 20 μm for each of the samples, and the images are shown in Fig. 4. The size of the grains increased, and the R_a decreased as the ratio of Cu to Ni decreased from 12:1 to 3:1 after the annealing treatment, as evidenced by signs of granular features on the surface of AFM images shown in Fig. 4. It appears that the annealing parameters here are acceptable for alloys rich in Ni but not yet optimized for alloys rich in Cu due to evaporation effects. The annealing process needs to be optimized in order to reduce the film roughness found in Cu rich alloys, such as the 12:1 CuNi samples. We are beginning to experiment with higher pressure during annealing to reduce the evaporation rate of Cu that we believe is causing the increased roughness.

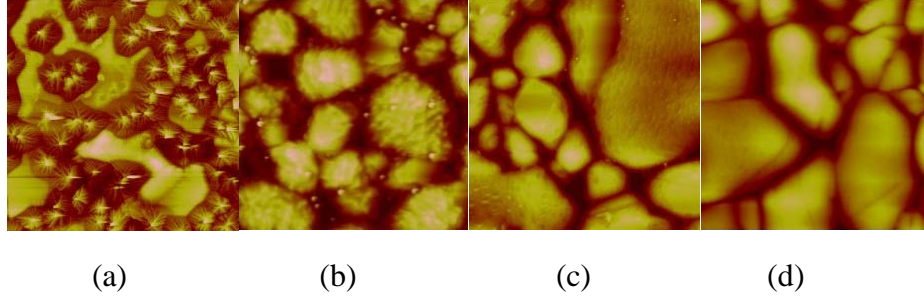


Fig. 4 AFM image and roughness measurement of a) 220 nm for 12:1, b) 86 nm for 6:1, c) 74 nm for 4:1, and d) 66 nm for 3:1 CuNi alloy

2.7 Uniformity of the Depositions

In order to verify the uniformity of the deposited films across a 100-mm-diameter wafer, we performed a quick and non-destructive test using an electrical 4-point probe measurement technique. We measured the electrical sheet resistivity of the deposited films across 25 equally separated points in a circular pattern around the wafer, from which we generated the contour map shown in Fig. 5 for 3:1 CuNi (sample S15). We calculated a uniformity of 94% using the equation:

$$Uniformity = \left(1 - \frac{std}{mean}\right) * 100. \quad (2)$$

The film uniformity for the deposited bilayer sample was excellent across a 100-mm-diameter substrate with the established sputtering parameters of 5-mT Ar pressure and 400 °C substrate temperature. The color bands in Fig. 5 represent sheet resistance (Ω/cm^2) values. The other film samples, S1–S16, also exhibited very similar calculated values for uniformity and reproducibility.

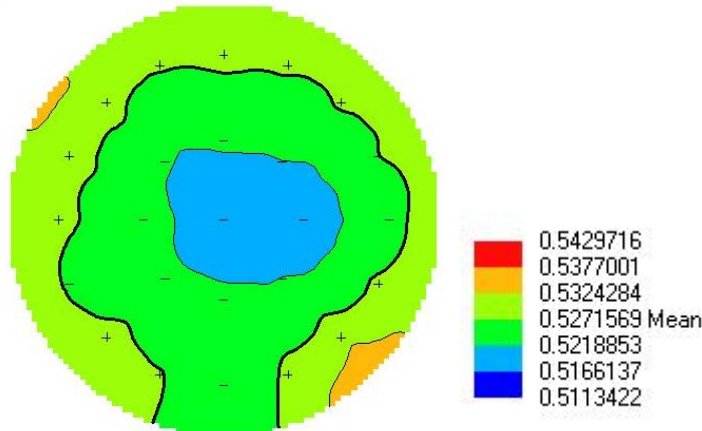


Fig. 5 Contour map showing measured electrical resistivity values across 25 points on a 100-mm-diameter substrate for 3:1 CuNi alloy

3. Conclusion

The AJA model ATC-2200 sputtering system can deposit films with a uniformity of 94% or better at a substrate distance of 100 mm. A substrate temperature of 250 °C was required to achieve films with a preferred (111) crystalline orientation after alloying of the samples. We demonstrated a simple and effective way to produce CuNi film alloy concentrations in the range from 90/10 to 70/30 at.% by varying the ratio of the initial deposited Cu and Ni layers.

4. References and Notes

1. Brodie I, Murray JJ. The physics of microfabrication. New York (NY): Plenum Press; 1982.
2. Chen A, Zakar E, Burke R. Preparation of copper (Cu)-nickel (Ni) alloy thin films for bilayer graphene growth. Adelphi (MD): Army Research Laboratory (US); 2016. Report No.: ARL-TR-7593.
3. Cullity BD. Elements of X-ray diffraction. Reading (MA): Addison-Wesley; 1978. p. 101–102.

List of Symbols, Abbreviations, and Acronyms

AFM	Atomic Force Microscopy
Ar	argon
at. %	atomic percent
C	carbon
CH ₄	methane
Cu	copper
EDX	Energy-Dispersive X-ray Spectroscopy
H ₂	hydrogen
LPCVD	Low Pressure Chemical Vapor Deposition
Ni	nickel
R _a	average roughness
vol. %	volume percent
XRD	X-ray Diffraction

1 DEFENSE TECHNICAL
(PDF) INFORMATION CTR
DTIC OCA

2 DIRECTOR
(PDF) US ARMY RESEARCH LAB
RDRL CIO L
IMAL HRA MAIL & RECORDS
MGMT

1 GOVT PRINTG OFC
(PDF) A MALHOTRA

40 DIRECTOR
(PDF) US ARMY RESEARCH LAB
RDRL SER E P AMIRTHARAJ
RDRL SER L B PIEKARSKI
RDRL SER E R DEL ROSARIO
RDRL SER L M DUBEY
RDRL SER L E ZAKAR
RDRL SER L B NICHOLS
RDRL SER L M CHIN
RDRL SER L M ERVIN
RDRL SER L R BURKE
RDRL SER L A MAZZONI
RDRL SER L S NAJMAEI
RDRL SER L A CHEN
RDRL SER L B ISAACSON
RDRL SER L C KNICK
RDRL SER L D JORDAN
RDRL SER L D POTREPKA
RDRL-SED L M ERVIN
RDRL SER L M SROUR
RDRL SER L R POLCAWICH
RDRL SER L R BENOIT
RDRL SER E G BIRDWELL
RDRL SER E F CROWNE
RDRL SER E P SHAH
RDRL SER E T O'REGAN
RDRL SER E T IVANOV
RDRL SER-E M DERENGE
RDRL SEE E R FU
RDRL SEE M SUNAL
RDRL SEG M ROY
RDRL SEG S STRNAD
RDRL SEG J MULCAHY
RDRL SEG N MARK
RDRL SEG W BERNARD
RDRL SED E A ROSENFELD
RDRL SED E V TSENG
RDRL SED C C RONG
RDRL SED C Z DUNBAR
RDRL SED E E KESSLER
RDRL SED E I KIERZEWSKI
RDRL SES P J TIMMERWILKE